Surface Science 641 (2015) 260–265

Contents lists available at ScienceDirect

Surface Science

journal homepage: www.elsevier.com/locate/susc

Diindenoperylene adsorption on Cu(111) studied with density-functional theory

H. Aldahhak *, E. Rauls, W.G. Schmidt

Lehrstuhl für Theoretische Physik, Universität Paderborn, 33100 Paderborn, Germany

ARTICLE INFO

Available online 19 March 2015

Keywords:
Cu(111)
Diindenoperylene
Adsorption
Ab initio
DFT

ABSTRACT

First-principles calculations on the adsorption of diindenoperylene molecules on Cu(111) are presented. Single molecules as well as molecular monolayers on planar surface have been studied in detail, both with respect to the adsorption structure and the modification of the molecular charge density. Among the geometries studied here, long-range ordered arrangements of DIP molecules are found to be most favorable.

The adsorption of the perylene-based diindenoperylene (DIP, $C_{32}H_{16}$) (Fig. 1a) on different substrates is of considerable interest for applications related to organic optoelectronic devices [1,2]. This is due in part to the ambipolar behavior of the molecules [3] and their thermal stability [4] as well as due to their ability to form well-ordered films on a variety of substrates [5–7]. Surface adsorbed DIP molecules form different superstructures depending on the substrate type and the growth conditions [8–17].

In case of DIP molecules adsorbed on Cu(111), different assembling patterns are found in dependence on the terrace width [9]. A well-ordered long-range order (LR) (Fig. 1b) is observed on narrow terraces (≤15 nm). In this case, the DIP molecules are arranged in unit cells of dimensions a = 8.7 ± 0.4 Å, b = 18.5 ± 0.7 Å, γ = 71 ± 1° and all molecules are co-directionally oriented. In contrast, on wide terraces (≥15 nm), DIP molecules adsorb in a short-range order (SR) with only few molecules adsorbed co-directionally within domains. These domains are oriented along the three equivalent directions determined by the hexagonal symmetry of the substrate (Fig. 1c). Normal incidence X-ray standing wave determination of the adsorbate-substrate distance yielded a value of 2.51 ± 0.03 Å for single DIP molecules adsorbed on Cu(111) [11]. From non-contact atomic force microscopy it was concluded that the geometries of the singly adsorbed DIP molecules slightly deviate from the planar form [11,12]. In these studies, the orientation and the registry of the molecules have not been determined.

Here we perform density-functional calculations on singly adsorbed DIP molecules as well as adsorbed monolayers, but restrict ourselves to the adsorption on planar surfaces. After a short description of the methodology, we first address the single molecule adsorption. Convergence tests with respect to the slab thickness and Brillouin-zone sampling are presented. The adsorption geometry and the charge redistribution upon adsorption are discussed and compared with the available experimental findings. Finally, the role of the molecule–surface and the molecule–molecule interactions in realizing different monolayer configurations is investigated.

Total-energy density functional calculations have been performed using the Vienna Ab Initio Simulation Package (VASP) [19]. The electron–ion interactions are described by the projector-augmented wave (PAW) method [20]. To model the electron–electron exchange-correlation energy, the generalized gradient approximation, specifically the PW91 [21] functional, was used. The ubiquitous dispersion interaction can be accounted for accurately by performing high-level quantum-chemical wave function or quantum Monte Carlo methods or by the combination of exact exchange plus correlation energy within the adiabatic-connection fluctuation-dissipation theorem. It is neglected by most of the currently used exchange-correlation functionals in DFT calculations, however. Among the many concepts to include dispersion interaction in DFT, the addition of a pairwise interaction energy $\sim C_6 R^{-6}$ with a suitable cutoff function for small atomic distances R (see, for example, Ref. [22]) is a computationally particularly inexpensive, still often rather accurate approach [23–28]. This so-called DFT-D scheme delivers information on the influence of van der Waals forces at virtually no additional computational costs and is employed here, using the parameters suggested by Schmidt and co-workers [22]. The Kohn–Sham orbitals are expanded in a plane-wave basis with an energy cut-off of 340 eV. A Γ-centered 2 × 2 × 1 k-point mesh has been employed to integrate the Brillouin zone. Supercells consisting of six atomic layers separated by a vacuum region of 30 Å were used to model the Cu(111) substrate. A lateral 9 × 8 periodicity was used to study the single molecule adsorption. Atomic structure relaxations were performed with convergence criteria of 0.03 eV/Å and 10^{-5} eV for the forces and the

* Corresponding author.

http://dx.doi.org/10.1016/j.susc.2015.03.007
0039-6028/

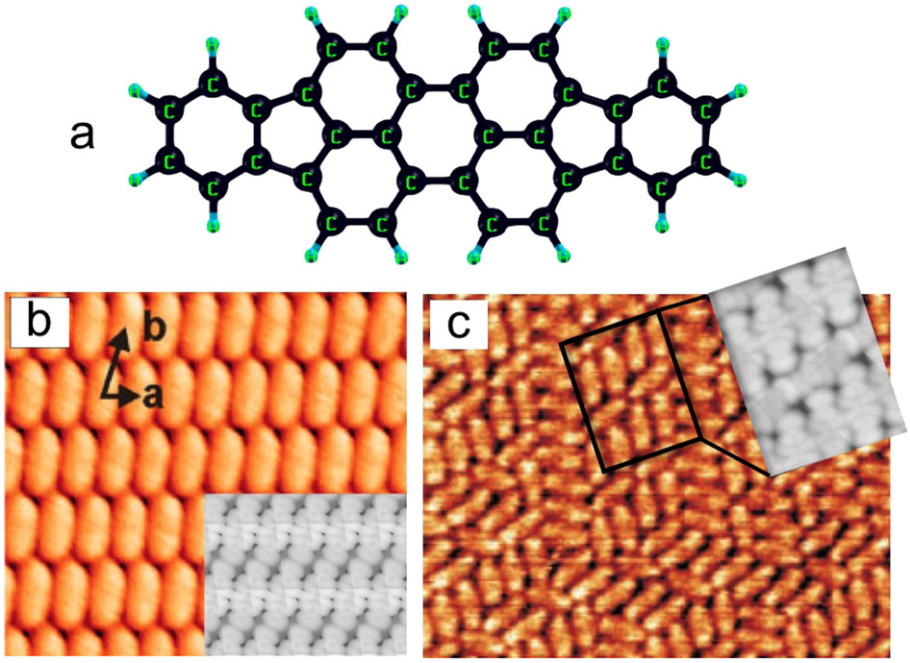

Fig. 1. (a) Ball-and-stick model of the DIP molecule. (b) The long-range (LR) and (c) the short-range (SR) arrangements of DIP molecules observed experimentally on Cu(111) [9]. Gray micrographs show STM simulations according to the Tersoff–Hamann model [18].

total energies, respectively. Thereby the structural degrees of freedom of the adsorbate atoms and the uppermost four substrate layers were relaxed, whereas the atoms in the bottom two atomic layers were fixed at the ideal bulk positions. Adsorption energies (E_{ads}) were calculated as

$$E_{ads} = E_{sys} - E_{sur} - E_{mol},$$

where E_{sys}, E_{sur} and E_{mol} are the respective energies of the adsystem, the clean surface and the gas-phase DIP molecule.

The variety of conceivable adsorption configurations studied here for single DIP molecules on the Cu(111) surface is shown in Fig. 2. The corresponding adsorption energies calculated for different slab thicknesses and k-point samplings are compiled in Fig. 3. Obviously, calculations for substrates modeled with four atomic layers do not lead to converged results. In this case, for example, the structure (h) is most favorable for a $(1 \times 1 \times 1)$ k-point grid, while structure (a) is most favorable when using a $(2 \times 2 \times 1)$ k-point sampling. Also the structural parameters are not fully converged for four-layer slabs. Using six-layer slabs leads to adsorption energies that have an error bar for relative adsorption energies that is below 0.1 eV. In this case also the energetic ordering of the adsorption structures does not depend on the k-point sampling anymore.

In its most stable adsorption structure (h), a single DIP molecule adsorbs with its long axis parallel to one of the three equivalent <121> orientations of Cu(111), while its center resides over a hollow site. Three out of its six inner carbon atoms (13, 17 and 18 in Fig. 4a) are located on top of surface Cu atoms. The other three inner carbon atoms (15, 16 and 20) are located on hollow sites of the surface. The outer rings (atoms 1 to 6 and 27 to 32 in Fig. 4a) have different registries with respect to the substrate. This results in a slightly asymmetric adsorption configuration, where, with respect to the center of the molecule, the C atoms on both sides of the molecule are lifted upwards by 0.12 Å and 0.4 Å. The slight asymmetry of the adstructure found here explains the small molecular torsion observed in Refs. [11,12]. For the adsorbate–substrate distances defined in Fig. 4b we calculate $d_{1/2} =$ 2.93/2.63 Å (distance between carbon atoms 1/2 (or 31/32) and the Cu atoms beneath) and $d_{b/c} =$ 2.48/2.54 Å (distance between carbon atoms 13/17 to the Cu atoms beneath). If one defines the height of the molecular center as average of d_c and d_b, the calculated distance between the center of the molecule and the surface fits perfectly to

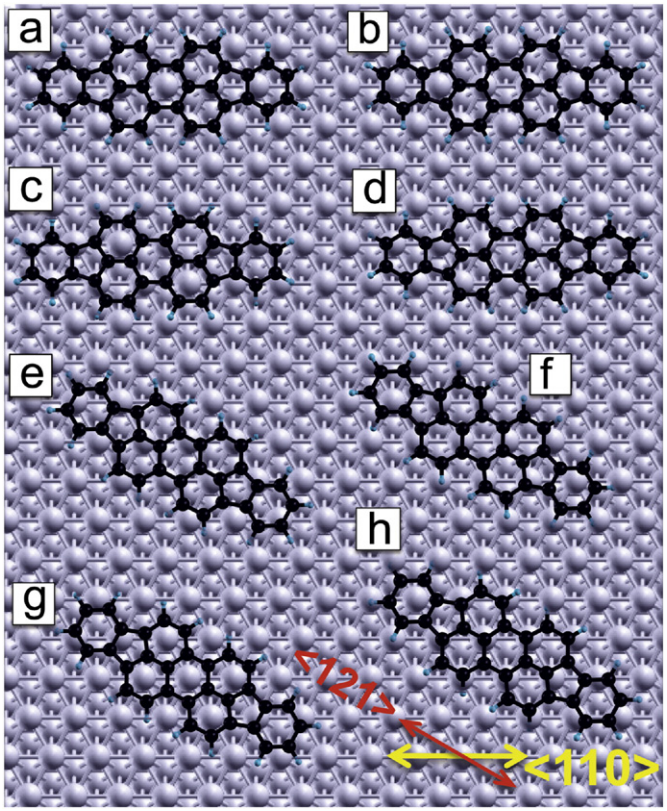

Fig. 2. Top views of different adsorption geometries of single DIP molecules on planar Cu(111). The long molecular axis is aligned parallel to one of the surface directions <10>, while the molecular center ring resides on (a) top, (b), (c) bridge, or (d) hollow positions. In the other structures, the molecules are directed along one of the <121> directions with the center ring in (e), (f) bridge, (g) top or (h) hollow positions.

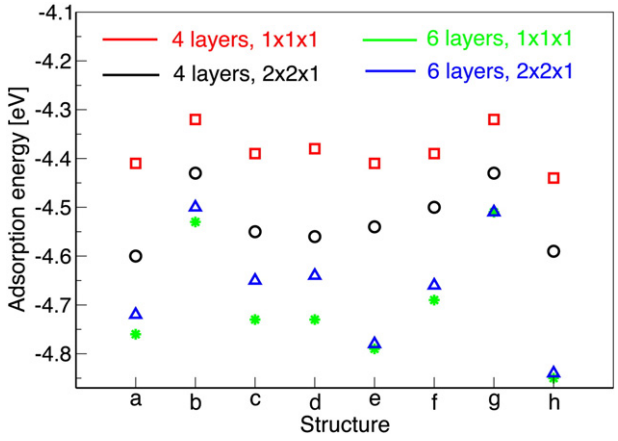

Fig. 3. Calculated adsorption energies for the structures defined in Fig. 2 in dependence on the k-point grid and the numbers of slab layers.

the experimental value of 2.51 Å [11]. The adsorption energy of structure (h) calculated here to be −4.84 eV is very close to the finding by Bürker et al. [11], who reported a value of −4.74 eV. This comparatively large adsorption energy is on the one hand simply related to the size of the molecule, but implies on the other hand a noticeable molecule–substrate interaction.

Table 1
Calculated DIP adsorption energies for various translational symmetries.

Unit cell	$\begin{pmatrix}8 & 4\\0 & 9\end{pmatrix}$	$\begin{pmatrix}4 & 2\\0 & 9\end{pmatrix}$	$\begin{pmatrix}8 & 4\\0 & 7\end{pmatrix}$	$\begin{pmatrix}6 & 3\\0 & 7\end{pmatrix}$	$\begin{pmatrix}4 & 2\\0 & 7\end{pmatrix}$
E_{ads} in eV	−4.82	−5.55	−5.05	−4.91	−5.49

In order to better understand this interaction, we calculated the charge redistribution upon adsorption. In Fig. 4a the charge accumulation and depletion in a plane 0.2 Å beneath the molecular center are shown. This is the plane where the total charge transfer is largest and corresponds to 0.34 e. Charge accumulation occurs mainly underneath the carbon atoms that are located directly above Cu atoms, e.g., atoms 12 and 14, while charge depletion can be observed at C atoms atop hollow sites, e.g., atoms 15, 16, and 20. The charge redistribution is stronger in the molecular center than at the outer atoms, and breaks the molecular symmetry, in accordance with the asymmetric bonding configuration. The slight asymmetry of the molecular polarization upon adsorption is also reflected in the simulated STM images. In Fig. 4c we show a STM simulation according to the Tersoff–Hamann method [18] for V = −1.5 eV and I = 0.05 mA. Because of the molecular asymmetric parabolic adsorption geometry, the two sides of the molecule look slightly brighter than its center, while one of them is brighter than the other.

Next we address DIP monolayers on Cu(111). In order to determine the energetically favorable thin film geometries, we calculated the adsorption energies for a variety of different molecular arrangements

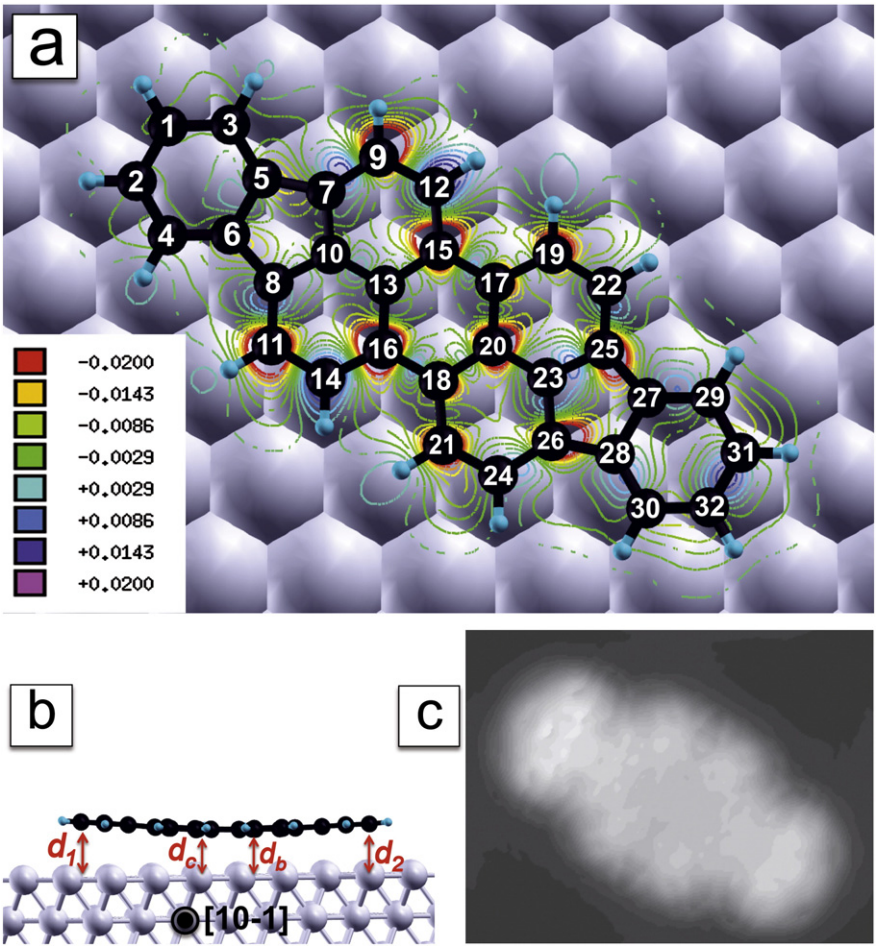

Fig. 4. (a) Top-view of the most favorable structure (h). Colored iso-lines indicate the calculated charge density redistribution upon adsorption. Positive (negative) values (in e/Å^3) indicate electron accumulation (depletion). (b) Side view of structure (h) and (c) its simulated STM micrograph (see text).

within different translational symmetries. The calculations show attractive molecule–molecule interactions. This can be seen from Table 1, where the calculated adsorption energy per molecule for different supercell sizes is given.

We obtained the highest adsorption energies of −5.63 eV and −5.76 eV for the two structures: phases A and B, respectively, shown in Fig. 5a, b. These two structures are characterized by a $\begin{pmatrix} A_1(B_1) \\ A_2(B_2) \end{pmatrix} =$

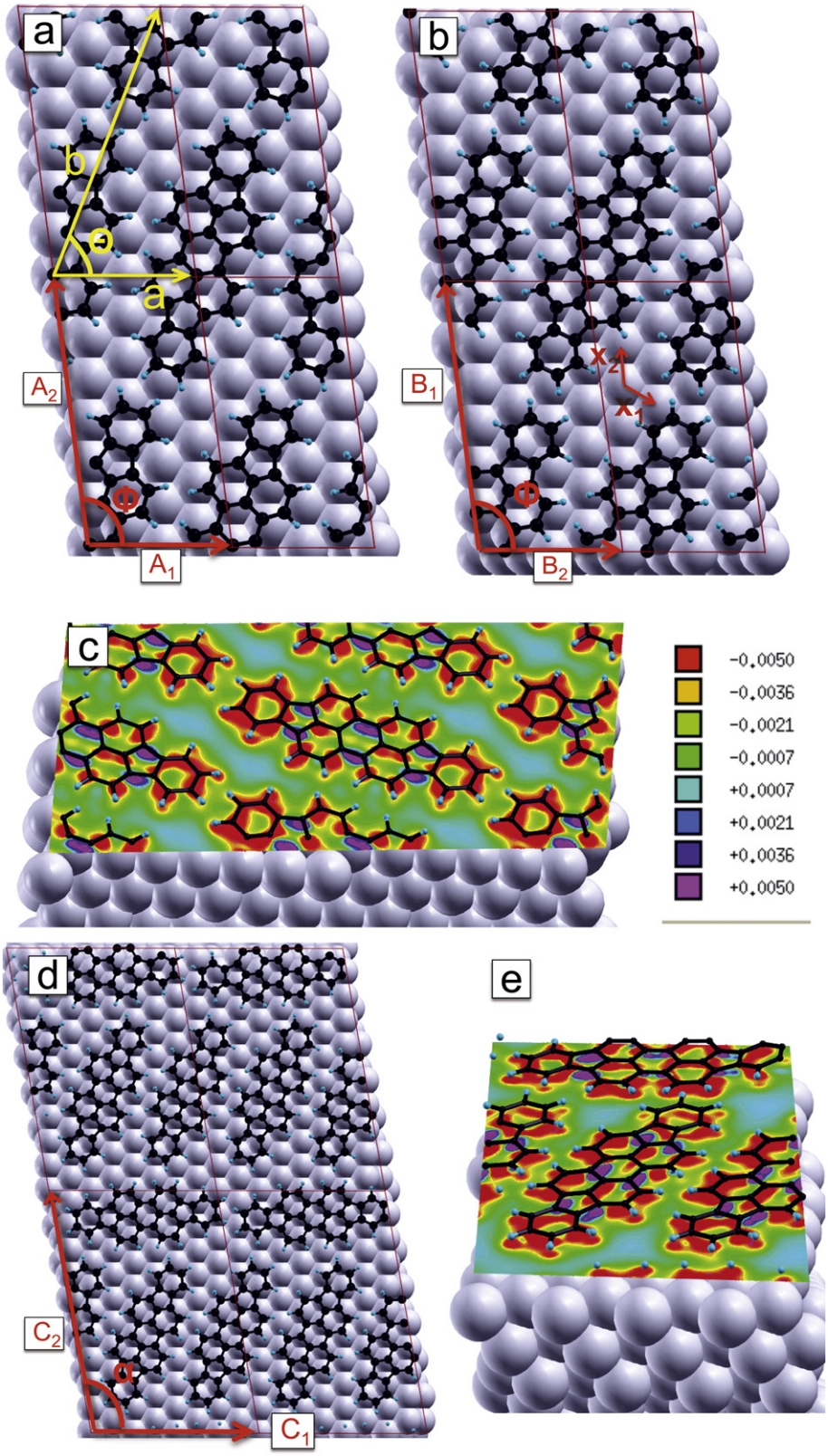

Fig. 5. Models of the most stable LR arrangements: phase A (a) and phase B (b) and the induced charge density (c) for Phase A. The SR order (d) with the induced charge density (e). The charge redistribution aspects are plotted on a plane located 0.4 Å below the molecular plane (see text).

$\begin{pmatrix} 4 & 2 \\ -1 & 6 \end{pmatrix}\begin{pmatrix} x_1 \\ x_2 \end{pmatrix}$ translational symmetry, where x_1 and x_2 are the primitive unit cell vectors of the Cu(111) surface. The dimensions are $A_1 = B_1 = 8.77$ Å, $A_2 = B_2 = 16.82$ Å, and $\Phi = 97.77°$, which correspond to a = 8.77 Å, b = 17.89 Å, and $\theta = 69.680°$ according to the notation used in Ref. [9], see red and yellow arrows in Fig. 5a. The dimensions of the calculated structures and the molecular arrangement within the surface unit cell are close to the LR structure observed in Ref. [9]. The molecular registries realized in the favorable monolayer structures identified here are similar to that of the singly adsorbed molecules. However, for steric reasons the molecular axis is rotated by 10° with respect to the $[1\bar{1}2]$ direction of the surface.

The most favorable thin film geometry calculated here that resembles the experimentally observed SR order is shown in Fig. 5d. It is characterized by three molecules within the surface unit cell of dimensions $C_1 = 17.61$ Å, $C_2 = 25.83$ Å, $\alpha = 99.96°$. The molecular axes of two molecules are azimuthally oriented in the same direction, whereas the third is rotated by 60° with respect to them. The molecular registries are similar to the LR arrangement. The adsorption energy per molecule for this structure amounts to −5.47 eV.

Comparing the LR and SR order structures with the single molecule adsorption, one finds that the molecule–molecule interactions lead to slight weakening of the molecule–surface interaction. That is reflected (i) in a slight charge redistribution from the region between the molecules and the substrate underneath towards the intermolecular region, see Fig. 5c and e, (ii) in a slightly increased molecule–surface distance which enlarges to about 2.9 Å as well as (iii) in the direct comparison of the molecule–surface interaction energies of the SR and LR order phases of about 4.5 eV (cf. Table 2) with the single molecule adsorption energy of about 4.8 eV.

A word of caution is in order concerning the adsorption energies calculated here for the SR and LR ordered adstructures: While reliable adsorption energies for single molecules can typically be obtained by a systematic scan of all conceivable adsorption geometries or the calculation of the potential energy surface, the situation is less comfortable for complicated adstructures in thin films. In the latter case the large number of structural degrees of freedom in conjunction with the large numerical expense of well-converged calculations regularly does not allow for the complete sampling of all possible structures. Therefore it cannot be excluded that configurations not considered in the calculations are even more favorable. In the present case we can certainly not exclude the occurrence of further, even more favorable LR and SR structures. Moreover, the present calculations neglect temperature effects. Vibrational and configurational entropy contributions to the surface free energy may modify the energetics at finite temperatures [29].

However, if one assumes the adsorption energies calculated here to describe the energy trend correctly, there seems to be an apparent contradiction with the experimental findings: While computationally the LR arrangement is most stable on the planar surface, experimentally an SR order is observed for wide terraces, see Ref. [9]. In this context it is helpful to quantify the molecule–surface and the molecule–molecule contributions to the adsorption energy. The calculated values for the LR structures A and B as well as the SR order structure are compiled in Table 2. It can be seen that the molecule–surface interactions are almost the same for all phases, and far stronger than the molecule–molecule interactions. This suggests the existence of a possibly long-lived metastable state that arises from the optimization of the molecule–substrate interactions: The molecules initially deposited on the surface are oriented according to the three discrete equivalent orientations of the surface. The energy barrier that needs to be overcome from this initial configuration towards formation of the SR order structure is lower than towards formation of the LR order structure, because in the latter case a collective rearrangement of many molecules is required. The hypothesis that the LR order is thermodynamically stable but its formation kinetically hindered is supported by very recent findings that show the co-existence of both LR and SR phases at the Cu(111) surface [30]. The fact that the LR order structure is formed on narrow terraces [9] indicates that step edges act as condensation nuclei of the LR order phase.

Table 2
A comparison between the molecule–surface (MS) and the molecule–molecule (MM) contributions to the calculated total adsorption energy in the LR and SR order adstructures.

Structure	LR A	LR B	SR
E_{ads} in eV	−5.63	−5.76	−5.47
MS in eV	−4.47	−4.50	−4.48
MM in eV	−1.16	−1.26	−0.99

In summary, DFT calculations on the adsorption of DIP on Cu(111) are presented that show an increase of the molecular adsorption energy by going from the single molecule case to short-range ordered and long-range ordered monolayer structures. The calculated adsorption geometries for single adsorbed molecules are in very good agreement with the experimental data available. The present finding that long-range order is energetically more favorable than short-range order does not contradict the experimental finding of short-range order on wide terraces: On the one hand temperature effects are not considered here, on the other hand the experimental observation may be related to a kinetically stabilized structure. This point of view is supported by most recent findings [30] that show a co-existence of both phases.

Calculations were performed at the Paderborn Center for Parallel Computing (PC^2). For financial support, the authors acknowledge the Deutsche Forschungsgesellschaft (D-A-CH project FWF I958 and GRK 1464).

References

[1] M.B. Casu, I. Biswas, B.-E. Schuster, M. Nagel, P. Nagel, S. Schuppler, T. Chassé, Appl. Phys. Lett. 93 (2008) 24103.
[2] J. Wagner, M. Gruber, A. Hinderhofer, A. Wilke, B. Bröker, J. Frisch, P. Amsalem, A. Vollmer, A. Opitz, N. Koch, F. Schreiber, W. Brütting, Adv. Funct. Mater. 20 (2010) 4295.
[3] A.K. Tripathi, J. Pflaum, Appl. Phys. Lett. 89 (2006) 082103.
[4] S. Sellner, A. Gerlach, F. Schreiber, M. Kelsch, N. Kasper, H. Dosch, S. Meyer, J. Pflaum, M. Fischer, B. Gompf, Adv. Mater. 16 (2004) 1750.
[5] A.C. Dürr, F. Schreiber, M. Munch, N. Karl, B. Krause, V. Kruppa, H. Dosch, Appl. Phys. Lett. 81 (2002) 2276.
[6] X.N. Zhang, E. Barrena, D.G. de Oteyza, E. De Souza, H. Dosch, J. Appl. Phys. 104 (2008) 104308.
[7] S. Kowarik, A. Gerlach, S. Sellner, F. Schreiber, L. Cavalcanti, O. Konovalov, Phys. Rev. Lett. 96 (2006) 125504.
[8] X.N. Zhang, D.G. de Oteyza, Y. Wakayama, H. Dosch, Surf. Sci. 603 (2009) 3179.
[9] D.G. de Oteyza, E. Barrena, H. Dosch, Y. Wakayama, Phys. Chem. Chem. Phys. 11 (2009) 8741.
[10] D.G. de Oteyza, J.M. García-Lastra, M. Corso, B.P. Doyle, L. Floreano, A. Morgante, Y. Wakayama, A. Rubio, J. Enrique Ortega, Adv. Funct. Mater. 19 (2009) 3567.
[11] C. Bürker, N. Ferri, A. Tkatchenko, A. Gerlach, J. Niederhausen, T. Hosokai, S. Duhm, J. Zegenhagen, N. Koch, F. Schreiber, Phys. Rev. B 87 (2013) 165443.
[12] B. Schuler, W. Liu, A. Tkatchenko, N. Moll, G. Meyer, A. Mistry, D. Fox, L. Gross, Phys. Rev. Lett. 111 (2013) 106103.
[13] H. Huang, J.-T. Sun, Y.P. Feng, W. Chen, A.T.S. Wee, Phys. Chem. Chem. Phys. 13 (2011) 20933.
[14] D.G. de Oteyza, E. Barrena, H. Dosch, J.E. Ortega, Y. Wakayama, Phys. Chem. Chem. Phys. 13 (2011) 4220.
[15] M.B. Casu, B. Schuster, I. Biswas, C. Raisch, H. Marchetto, T. Schmidt, T. Chassé, Adv. Mater. 22 (2010) 3740.
[16] D.G. de Oteyza, E. Barrena, M. Ruiz-Osés, I. Silanes, B.P. Doyle, J.E. Ortega, A. Arnau, H. Dosch, Y. Wakayama, J. Phys. Chem. C 112 (2008) 7168.
[17] M.B. Casu, S.-A. Savu, B.-E. Schuster, I. Biswas, C. Raisch, H. Marchetto, T. Schmidt, T. Chassé, Chem. Commun. 48 (2012) 6957.
[18] J. Tersoff, D.R. Hamann, Phys. Rev. B 31 (1985) 805.
[19] G. Kresse, J. Furthmüller, Comput. Mater. Sci. 6 (1996) 15.
[20] G. Kresse, D. Joubert, Phys. Rev. B (1999) 59.
[21] J.P. Perdew, J.A. Chevary, S.H. Vosko, K.A. Jackson, M.R. Pederson, D.J. Singh, C. Fiolhais, Phys. Rev. B (1992) 46.
[22] F. Ortmann, F. Bechstedt, W.G. Schmidt, Phys. Rev. B 73 (2006) 205101.
[23] E.R. McNellis, J. Meyer, K. Reuter, Phys. Rev. B 80 (2009) 205414.

[24] C. Thierfelder, M. Witte, S. Blankenburg, E. Rauls, W.G. Schmidt, Surf. Sci. 605 (2011) 746.
[25] E. Rauls, T. Pertram, W.G. Schmidt, K. Wandelt, Surf. Sci. 606 (2012) 1120.
[26] H. Aldahhak, E. Rauls, W.G. Schmidt, Surf. Sci. (2015)http://dx.doi.org/10.1016/j.susc.2015.01.013 (In Press).
[27] H. Aldahhak, W.G. Schmidt, E. Rauls, Surf. Sci. 617 (2013) 242.
[28] Q. Guo, A. Paulheim, M. Sokolowski, H. Aldahhak, E. Rauls, W.G. Schmidt, J. Phys. Chem. C 118 (2014) 29911.
[29] S. Wippermann, W.G. Schmidt, Phys. Rev. Lett. 105 (2010) 126102.
[30] H. Aldahhak, S. Matencio, E. Barrena, C. Ocal, W.G. Schmidt, E. Rauls, Phys. Chem. Chem. Phys. (2015)http://dx.doi.org/10.1039/C4CP05271D (In Press).